Accepted Manuscript

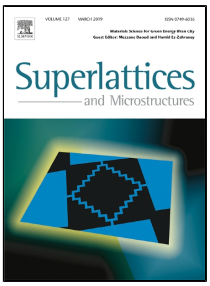

Edge functionalization of finite graphene nanoribbon superlattices

Hazem Abdelsalam, Vasil A. Saroka, Waleed Othman Younis

PII:	S0749-6036(18)32310-3
DOI:	10.1016/j.spmi.2019.03.008
Reference:	YSPMI 6045
To appear in:	*Superlattices and Microstructures*
Received Date:	16 November 2018
Accepted Date:	08 March 2019

Please cite this article as: Hazem Abdelsalam, Vasil A. Saroka, Waleed Othman Younis, Edge functionalization of finite graphene nanoribbon superlattices, *Superlattices and Microstructures* (2019), doi: 10.1016/j.spmi.2019.03.008

Edge functionalization of finite graphene nanoribbon superlattices

Hazem Abdelsalam[1], Vasil A. Saroka[2,3], Waleed Othman Younis[4]

[1]Theoretical Physics Department, National Research Centre, Giza, 12622, Egypt
[2]Institute for Nuclear Problems, Belarusian State University, Bobruiskaya 11, 220030 Minsk, Belarus
[3]Center for Quantum Spintronics, Department of Physics, Norwegian University of Science and Technology, NO-7491 Trondheim, Norway
[4]Vice Presidency for Postgraduate Studies and Scientific Research, Imam Abdulrahman Bin Faisal University, P.O. Box 1982, Dammam 31441, Saudi Arabia

ABSTRACT

The effect of chemical functionalization on the electronic properties of graphene nanoribbon superlattices with zigzag and armchair terminations is investigated using the density functional theory. ***The calculated positive binding energies imply that all the considered structures are stable before and after chemical modifications.*** The superlattices with armchair edges are characterized by a wide energy gap while those with zigzag edges have a narrow energy gap. The energy gap in superlattices with armchair edges nearly independent of their length while it strongly decreases and almost closes in superlattices with zigzag edges. The energy gap is comparably sensitive to the width variations in both types of the superlattices. It was found that the electric dipole moment increases with increasing the width in the case of armchair while it oscillates in zigzag superlattices. The electric dipole moment can be enhanced by chemical functionalization with COOH and NH2 groups. The effect of this functionalization is moderate for the energy gap, but the adsorption of tetracyanoquinodimethane transforms the system from insulator (E_g=2.66 eV) to a narrow band gap semiconductor (E_g=0.25 eV). The adsorption energy of tetracyanoquinodimethane and tetrathiafulvalene molecules can be enhanced by chemical functionalization which makes graphene superlattices useful for sensor applications and wastewater treatment.

Keywords: Graphene nanoribbons, Superlattices; ***Density functional theory (DFT)***; Chemical functionalization; Electronic properties; Molecular adsorption.

1. INTRODUCTION

Nowadays quasi-one-dimensional carbon nanostructures called graphene nanoribbons can be produces by a variety of methods such as ***chemical vapor deposition (CVD)*** growth [1], epitaxial side wall growth [2], nanolithography [3], plasma etching [4], self-assembling of molecular precursor [5] or wet synthesis [6]. Among these techniques the self-assembling stands out for its ability to produce structures with fascinating complexity and yet atomic precision [7]. The development of this technique has triggered a theoretical research on electronic [8], magnetic [9], optical [10] and transport [11] properties of so-called chevron-type ribbons or graphene nanowigglers. Due to the same reason a class of zigzag-shaped graphene nanoribbons superlattices garnered attention and received an impulse of development. The first theoretical study by Wu and Zheng [12] was inspired by pre-self-assembling attempts in producing ultra-smooth graphene edges [13]. Then, using first principles calculations, Cuong at el. [14] studied the energetic and electronic properties of zigzag-shaped superlattices with pure zigzag and mixed (zigzag and armchair) edges and reported their stability and the absence of the edge states at the corners of such structures. In the tight-binding model, the electronic properties of the structures with 60° and 120° angles and pure zigzag and armchair terminations have been reported for both cases without [15] and with [16] external electric field. In addition to the asymmetric superlattices consisting from two fragments of straight ribbons of unequal lengths [15,16], a generalization of the zigzag-shaped ribbon to the case when it consists of two straight fragments of unequal width has also been proposed and the band gap dependence on these parameters has been explored [17]. Within extended tight-binding model Szczęśniak et al. [18] have investigated 120° and 150° zigzag-shaped ribbons with equal lengths of straight fragments and reported the band gap dependence as a function of corner-corner distance that was in good agreement with the first principles results in Ref. [14]. In all these works, the ribbons are considered as being infinitely long. In reality, however, all self-assembled graphene nanoribbon samples are characterized by the distribution of finite lengths [5,19,20]. Therefore, revealing the effect of length is of great importance. ***Lately, we investigated the optical absorption [21] in finite-length self-assembled graphene nanoribbon superlattices produced in [19]. We found that in the 25 nm long nanoribbons the low-energy optical selection rules of infinitely long nanoribbons are well reproduced. Additionally, the density functional theory calculations of the band gap of ultra-short clusters have shown good agreement with the experimental results in Ref. [22].*** The rapid and quite successful development of molecular self-assembling approach has led to synthesis of the graphene nanoribbon superlattices not only on surface of the noble metals [5,23] but also in liquid solutions [24–26]. This allows one to transfer such structures to different substrates as well as to conveniently functionalize their edges with different functional groups [27]. The purpose of the present research is to investigate the effect of length in greater detail and reveal the influence of chemical functionalization on ribbons stability, electronic properties, chemical activity and intrinsic ***electric*** dipole moment. ***This is crucial for a number of recently proposed applications, for instance gas sensing [26], nanophotonics [28-30], digital electronics [31-33] and quantum information [34].*** In what follows, we present the structures in question and details of the computation model in Section 2, present and discuss results in Section 3 and provide summary in Section 4.

2. ATOMIC STRUCTURE COMPUTATIONAL MODEL

In this paper, we adopted the structure description developed in Refs. [15–17,35]. In brief, the unit cell of the superlattice is determined by a trio of chief vectors $\mathbf{L}_1$, $\mathbf{L}_2$ and $\mathbf{W}$. The first two vectors specify the edge profile, while the third one defines the width of the structure. Being crystal vectors of graphene hexagonal lattice the chief vectors can be factorized into a product of some integer and an elementary vector: $\mathbf{C} = d\,\mathbf{v}$, where $\mathbf{C}$ stands for any crystal vector of hexagonal graphene lattice, d is the integer, $\mathbf{v}$ is the elementary vector. Then the set of the elementary vectors $\mathbf{l}_1$, $\mathbf{l}_2$ and $\mathbf{w}$ uniquely identifies the superlattice type, whereas the set of three integers (ℓ_1, ℓ_2, w) determines the particular structure within this type. By using this approach the atomic coordinates of the unit cell can be generated [36]. The finite length structure is produced by translating the generated unit cell certain number of times by the superlattice translation vector $\mathbf{T}$. Thus, similar to previous research [37], the length in determined by the number of unit cells in the given structure. That is why we supplement the standard superlattice notation by additional label: L<number of unit cells>, where L stands for "length". The constructed nanoribbon superlattices are then converted to Gaussian09 [38] input files to perform ***the density functional theory (DFT)*** calculations [39,40]. The Becke-threeparameters-Lee-Yang-Parr hybrid functional (B3LYP) [41,42] is employed to calculate the electronic properties of the selected supercells. The 3-21g basis set is adopted in our calculation which has shown adequacy in size with respect to larger basis such as 6-31g [43,44].

3. RESULTS AND DISCUSSION

For the model study, we select superlattices with the apex angle equal to 120 degrees. These structures are found to be more stable as compared to the others characterized by different apex angles or even straight edges [14]. In what follows, we choose for the model study structures with ℓ_1 and ℓ_2 indexes equal to 3. Therefore, for structures A120 (3,3,1)L1 we simplify notation as A120(1)L1. Similar convention applies to the superlattices with zigzag edges. Namely, Z120(w)Lℓ stands for Z120(3,3, w)Lℓ which means that the width index of the structure is equal to w, while the length of the structure is equal to ℓ elementary translation periods.

3.1. HYDROGENATED NANORIBBON SUPPERCELLS

In this subsection we study the optimized structure and the electronic properties of armchair and zigzag nanoribbon superlattices with different lengths and widths. Fig. 1 presents the optimized structures of various superlattices, from A120(1)L1 to A120(1)L3 and A120 (1)L1 to A120 (3)L1 for armchair nanoribbons, and similarly for zigzag ones, to show the effect of increasing the length or the width of the nanoribbons on their stability and electronic properties. The binding energy is calculated to study the stability of the present nanoribbon superlattices; it is defined as the total energy of carbon atom multiplied by the total number of C-atoms plus the total energy of hydrogen atom multiplied by the total number of H-atoms minus the total energy of the hydrogenated superlattice. It is found that the binding energy (E_B), and therefore structure stability, increases with increasing the length or the width as given in Table l. However, the increment in the binding energy due to increasing width as in Fig. 1 (a), (e), and (h) is considerably higher that its increment due to the increase in the length as shown in Fig. 1 (a), (b), (c), and (d). The bond length between carbon atoms in armchair nanoribbons ranges from 1.34 to 1.50 Å while in zigzag ones this range is 1.35-1.48 Å. The long bonds that are observed at the edges of the supercells are

different from the C-C bond length (d_{cc}=1.42 Å) in infinite graphene by 4.2% in zigzag and 5.6% in armchair structures. These values are slightly higher than the 3.5% reported for infinitely long armchair ribbons in Ref. [45].

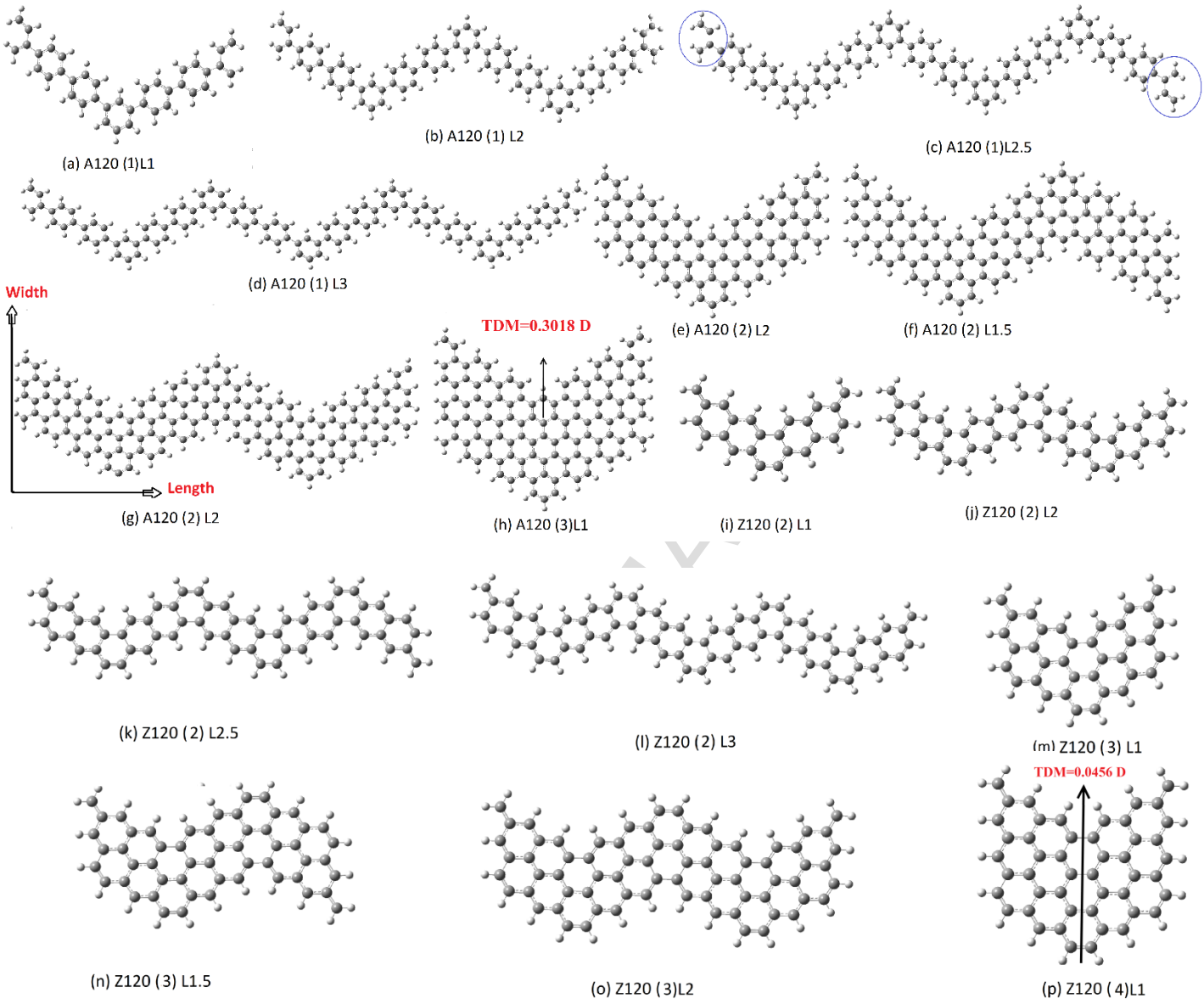

Fig. 1 The optimized structures of various hydrogenated armchair (a-h) and zigzag (i-p) nanoribbon supercells.

Let us now consider the electronic properties of the selected systems. It is clearly seen from Table 1 and Fig. 2 (c) that the armchair clusters are characterized by a wide energy gap. The gap gently decreases as the superlattice cluster length increases, namely E_g=3.88 eV in A120(1)L1 and E_g=3.81 eV in A120(1)L3 as shown by filled squares in Fig. 2 (a). However, upon increasing the width index w from 1 to 3, as shown in Fig. 1 (a), (e), and (h), the energy gap drops from 3.88 to 2.1 eV (see filled circles in Fig. 2 (a)). The situation is completely different in zigzag superlattices. The narrow energy gap of about 1.13 eV for Z120(2)L1 in Table 1 rapidly decreases with increasing length index ℓ (by 1 or 0.5 corresponding to 1

and 0.5 translation vectors) and moderately decreases with increasing width index w. This effect is especially well seen in panel (b) of Fig. 2.

In order to understand better the origin of the wide/narrow energy gap in armchair/zigzag nanoribbon superlattices and the gap behavior for increasing ℓ and w in both types of the superlattices, we calculated their electronic energy levels. We also calculated the electronic wave functions to reveal the nature of the highest occupied molecular orbital (HOMO) and the lowest unoccupied molecular orbital (LUMO). As seen from Fig. 2 (c) and (d), the A120(1)L3 superlattice has a wide energy gap of about 4 eV, whereas Z120(2)L3 has a tiny E_g=0.09 eV due to the appearance of two energy states inside the size gap region. Note, however, that $E_{size,g}$=3.1 eV that is comparable to the E_g in A120(1)L3 superlattice. The HOMO and LUMO in A120(1)L3 are different, as shown in Fig. 2 (e). ***The HOMO is distributed in the center of the nanoribbon, while the LUMO distributes only over the arms, both of them are antisymmetric (i.e. there is a mirror symmetry with respect to the vertical line passing via center of the structure up to phase factor equal to π) and π-bonding orbitals.*** The HOMO and LUMO of p-electron nature in Z120(2)L3 are localized at the ends of the finite superlattice rather than edges as in finite zigzag graphene quantum dots [46], infinitely long zigzag nanoribbons [47,48], or zigzag-shaped superlattices [14]. As one can see from Fig. 2 (f), the major parts of the HOMO and LUMO wave functions in Z120(2)L3 are localized within $|\mathbf{T}|/2$ distance from the structure ends. It should be noticed that similar to A120(1)L3 the HOMO of Z120(2)L3 is antisymmetric. At the same time, the LUMO is symmetric since there is the mirror symmetry with respect to the vertical line passing via center of the structure.

Table 1. The binding energy (E_B), the energy gap (E_g), and ***the total electric dipole moment (TEDM)*** of the optimized armchair (A120) and zigzag (Z120) graphene superlattices at the b3lyp/3-21g level of theory.

	Structure	d_{CC} (Å)	E_B(eV)	E_g (eV)	TEDM (D)
A120	A120 **(1)**L1	1.34-1.50	6.119	3.845	0.0039
	A120 (1)L2	1.34-1.50	6.255	3.819	0.0054
	A120 (1)L2.5	1.34-1.50	6.284	3.813	0.0001
	A120 (1)L3	1.34-1.50	6.319	3.809	0.0014
	A120 **(2)**L1	1.34-1.49	6.993	2.674	0.1468
	A120 (2)L1.5	1.34-1.49	7.116	2.665	0.0000
	A120 (2)L2	1.34-1.49	7.182	2.658	0.1490
	A120 (2)L2.5	1.34-1.49	7.223	2.653	0.0001
	A120 **(3)**L1	1.34-1.49	7.388	2.104	0.3018
Z120	Z120 **(2)**L1	1.35-1.48	6.3528	1.13	0.1592
	Z120 (2)L2	1.35-1.48	6.5745	0.19	0.1747
	Z120 (2)L2.5	1.35-1.48	6.6243	0.12	0.0000
	Z120 (2)L3	1.35-1.48	6.6584	0.09	0.1758
	Z120 **(3)**L1	1.36-1.48	6.7932	0.52	0.1216
	Z120 (3)L1.5	1.36-1.48	6.9733	0.21	0.0005
	Z120 (3)L2	1.36-1.48	7.0704	0.14	0.1344
	Z120 (3)L2.5	1.36-1.48	7.1307	0.102	0.0002
	Z120 **(4)**L1	1.36-1.48	7.0552	0.3559	0.0456

These orbitals are of the antibonding π-type, they have high energy and loosely bound to the structure. Therefore, zigzag nanoribbons superlattices must be highly interactive with the surrounding medium through its ends whereas the most interactive sites in armchair ones are situated in their center. The interactivity also enhances with increasing ***the total electric dipole moment (TEDM)*** of the system. The ***TEDM*** for various armchair and zigzag nanoribbons superlattices are given in Table. 1. The value of ***TEDM*** in A120 structure increases with increasing the width w, while, in deep contrast, it decreases in the Z120 structure. In armchair superlattices increasing the width leads to the increase of the number of C-H bonds in the width direction. As seen in Fig. 1 (g) the local dipoles generated from these bonds increase the total dipole in the width direction, namely from ***TEDM***=0.0039 D in A120(1)L1 to 0.3018 D in A120(3)L1. These values seem to be rather small, however, if we passivate the edges with fluorine that have high electronegativity with respect to carbon, the ***TEDM*** attains value of 1.57 D in A120 (1) L1 and 1.97 D in A120(3)L3. For the zigzag case, the additional C-H bonds are aligned horizontally as seen in Fig. 1 (o) with little tilting in the negative width direction. Therefore, the local dipoles from these additional bonds decrease the total dipole in the width direction as seen in Fig. 1 (p). Further increase in the zigzag superlattice width results in a minimum ***TEDM*** in the opposite direction (***TEDM***= 0.029 D in Z120(5)L1). Then the magnitude increase in the other direction (***TEDM***= 0.2989 D in Z120(6)L1) and so on (***TEDM***= 0.0632 D in Z120(8)L1) leading to an oscillation in the magnitude and direction of ***TEDM*** with increasing the width. Moreover, the ***TEDM*** almost vanishes in half-length cases in both armchair and zigzag regardless of the width, such as A120(1)L2.5 and Z120(3)L1.5. This effect can be explained in terms of the edge atoms (see the encircled atoms in Fig. 1 (c)) where in the case of A120 (1) L2.5 the local dipoles from the upper encircled bonds cancel those dipoles from the lower ones.

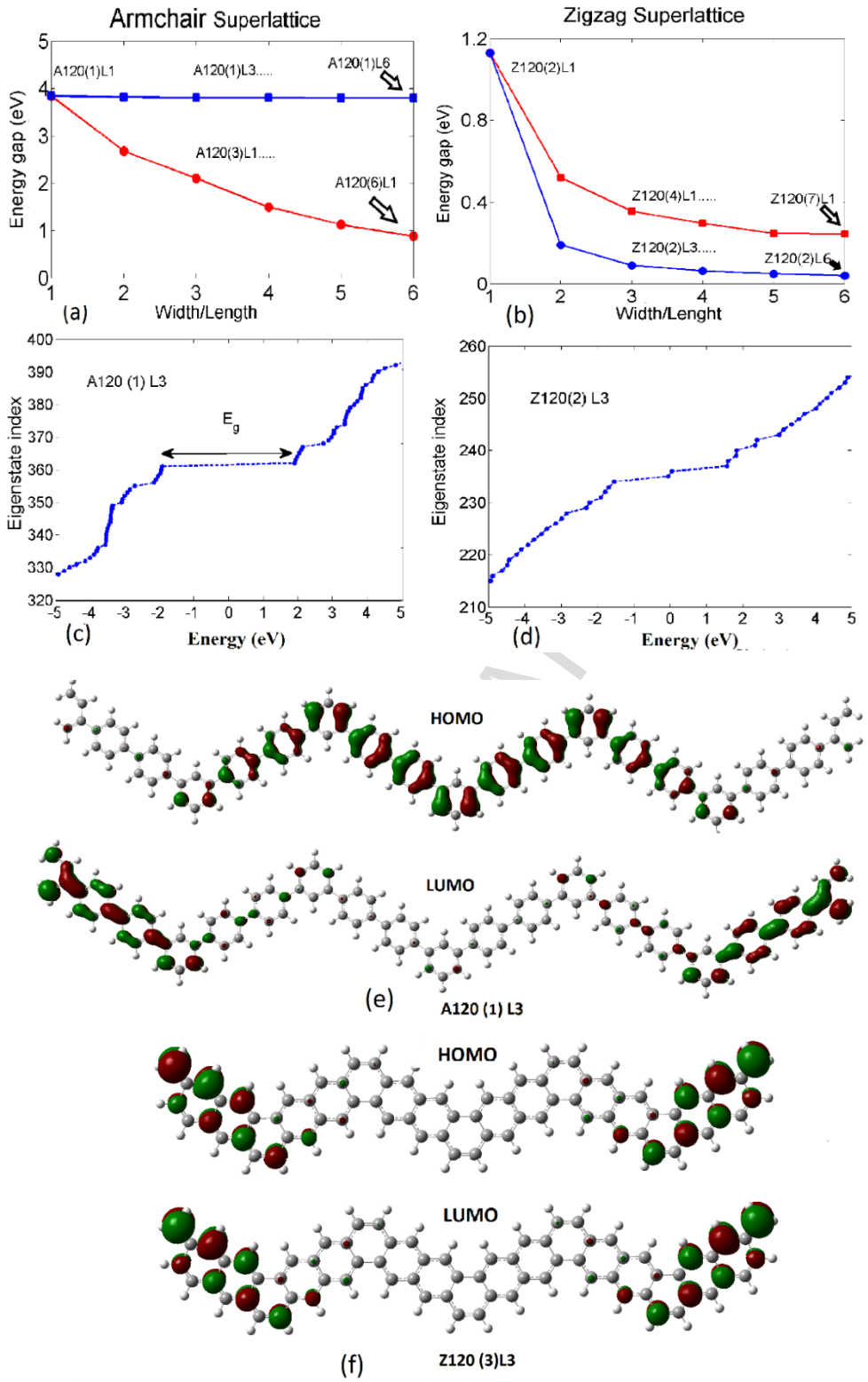

Fig. 2 The electronic properties of A120 and Z120 finite-length superlattices: (a), (b) the energy gap dependence on the width and length of A120 and Z120 structures; (c), (d) the electronic energy levels and (e), (f) the corresponding HOMO/LUMO of A120(1)L3 and Z120(2)L3 superlattices, respectively.

3.2 FUNCTIONALIZED GRAPHENE NANORIBBON SUPERCELLS

In this subsection, we consider the effect of edge functionalization on the energy gap and the total electric dipole moment of armchair and zigzag superlattices having width index $w = 2$ and length index $\ell = 2$. The chemical groups considered here are CH3, CHO, CN, COCH3, COOH, NH2, and OH. The groups are attached as shown in Fig. 3. This figure shows selected groups that are useful for the discussion on the dipole moment. The stability analysis in Gaussian 09 package resulted in only positive frequencies thereby confirming stability of the finite-length graphene nanoribbon superlattices under different functionalization. The lengths (d_{XC}) of bonds between the attached groups and the edge carbon atoms are given in Table. 2. The first d_{xc} value in Table 2 corresponds to the length of the bond between the chemical group and the outer edge atoms of the supercells (they are almost the same). The second d_{xc} value in Table 2 represents the length of the bond between the attached group and the carbon edge atom at the center of the superlattice. The variations in the energy gap and total electric dipole moment due to the attachment of all groups are given in the fourth and fifth columns of Table. 2, respectively. It must be noted that the effect on the energy gap in both armchair and zigzag cases is negligible. However, their effect on the ***TEDM*** is significantly higher, namely dipole moments up to 18.43 D (armchair) and 13.23 D (zigzag) are obtained by attaching COOH and CN groups to the edges of the superlattice, respectively. It worth noting that, the attachment of CN groups to graphene quantum dots also provides a considerable enhancement to the ***TEDM*** [49].

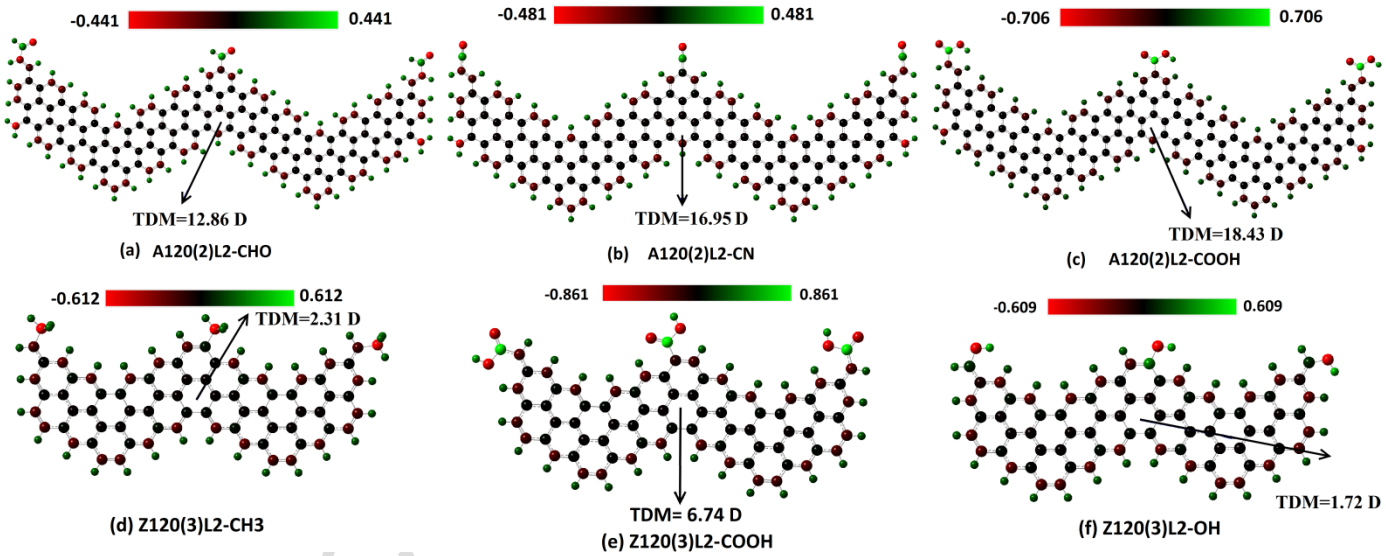

Fig.3 The optimized structures, charge distribution, and the total dipole moment of A120 and Z120 nanoribbons superlattices functionalized with different chemical groups.

The attachment of COOH produces giant dipole ***TEDM***=18.43 D in A120 structures and a moderate ***TEDM***=6.74 D in Z120 structures. In the case of attaching COOH to A120(2)L2 (see Fig. 3 (c)) the large local dipole moments from the C=O and C-O in the COOH group sum up in *y*-direction yielding total *y*-dipole moment=16.6 D and the O-H bond results in a net *x*-dipole moment=8 D. The *x*- and *y*-dipole moments sum up to the ***TEDM***=18.43 D in the direction shown in Fig. 3 (c). In the case of attaching COOH to Z120(3)L2 superlattice (Fig. 3 (e)), the bonding between COOH and the edge atoms takes an orientation in which total dipole moments in *x*- or *y*-directions dramatically decrease to 6.74 D because of

the cancelation of some local dipoles. Thus, one can see the edge termination affects significantly the total electric dipole moment and plays an important role in controlling TEDM value. We have seen that among the selected groups CN and COOH groups provide the largest enhancement of the ***TEDM***. Due to the high electronegativity of O and N compared to that of C, the groups containing C-O and C-N bonds have high electric dipole moments. The small difference between the electronegativity of C and H atoms in groups with C-H bonds like CH3 leads to a small net dipole moment.

Table 2. The bond length between the attached group and the superlattice edge atoms (d_{xc}), the energy gap of the functionalized system (E_g) and the total electric dipole moment (***TEDM***) for A120 and Z120 structures functionalized with different chemical groups.

Structure		**d_{XC} (Å)**	**E_g (eV)**	**TEDM (D)**
A120(2)L2	CH3	1.51, 1.52	2.6904	2.3808
	CHO	1.47, 1.48	2.5399	12.8469
	CN	1.42, 1.43	2.5845	16.9497
	COCH3	1.48, 1.50	2.6525	10.2498
	COOH	1.48, 1.50	2.5709	18.4264
	NH2	1.37	2.53339	11.8837
	OH	1.38, 1.39	2.6697	4.6183
Z120(3)L2	CH3	1.50, 1.52	0.134	2.3110
	CHO	1.44, 1.47	0.130	9.2917
	CN	1.39, 1.42	0.129	13.2276
	COCH3	1.45, 1.50	0.130	6.5110
	COOH	1.44, 1.48	0.129	6.7361
	NH2	1.36, 1.37	0.151	11.6247
	OH	1.37, 1.38	0.137	1.7184

The effect of chemical modification on the band gap can be enhanced through the adsorption of typical organic molecules such as tetracyanoquinodimethane (TCNQ) and tetrathiafulvalene (TTF) on the edges. These molecules have shown strong ability to drastically change the electronic properties of graphene and phosphorene sheets when adsorbed on them [50,51]. Fig. 4 presents our proposition for the adsorption process of these molecules on the edges of the graphene superlattices to disclose the effect of adsorption on the electronic properties and the effect of chemical functionalization on the adsorption itself. Once these molecules are placed at distance 6 Å from the core edge atom as shown in Fig. 4 (a), the minimum energy configuration and adsorption site are obtained by performing the DFT optimization. The adsorption of TCNQ (TTF) on the edges of the hydrogenated A120 cluster, Fig. 4 (a-e), dramatically decreases the energy gap from 2.66 to 0.25 (0.7) eV. Such decrease has not been achieved by attaching any of the other considered chemical groups. This small energy gap persists even when the A120 superlattices are functionalized by COOH groups (see Fig. 4 (d), (e)) but it slightly increases to 0.27 and 0.8 eV for the adsorption of TCNQ and TTF, respectively. In the case of TCNQ and TTF adsorption on Z120 superlattices, the energy gap is almost the same as before adsorption, namely E_g~ 0.14-0.15 eV after the adsorption. It is worth noting that the energy gap in Z120 superlattices-TCNQ has a negative value (E_g~ -1.35 eV) because the HOMO has higher energy than the LUMO which means that the resultant

structure is a semimetal. This structure transformed to semiconductor with E_g= 0.15 eV by attaching three NH2 groups to the edges.

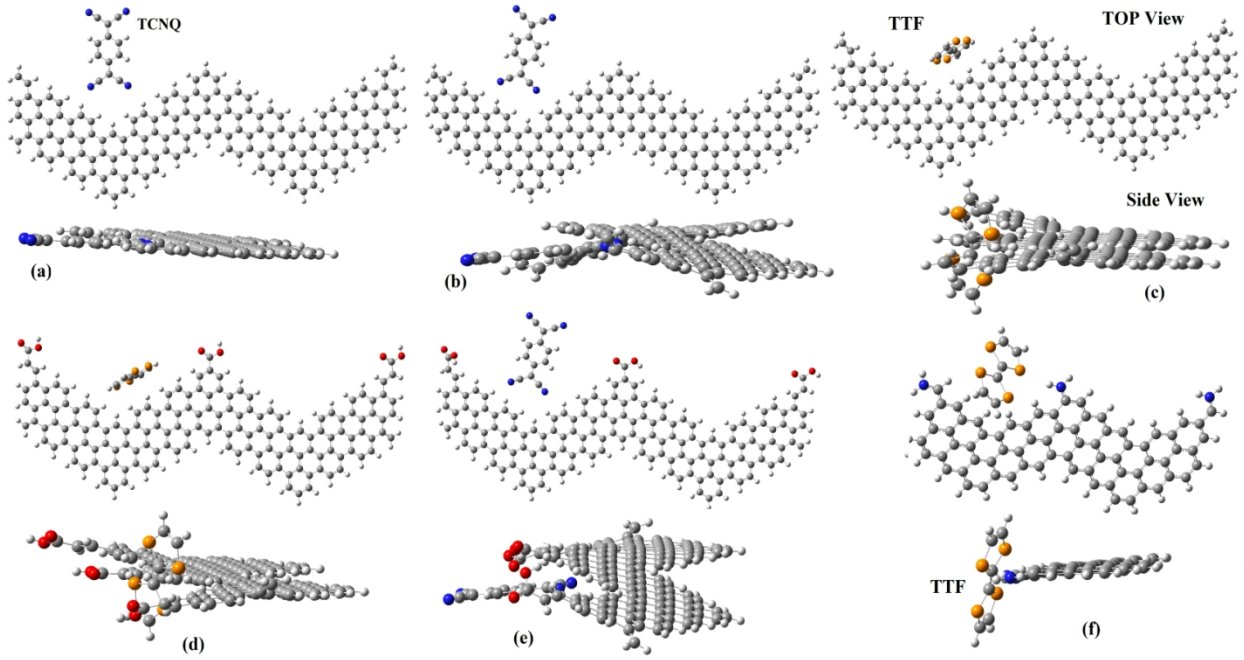

Fig. 4. (a) Initial configuration of the adsorption of TCNQ by A120(2)L2, (b) the corresponding optimized structure, and (c) the optimized structure of TTF adsorbed by the A120(2)L2 . Adsorption of TTF and TCNQ by 3COOH-functionalized A120(2)L2, (d) and (e) respectively. (f) TTF adsorption on the edges of Z120(3)L2.

The adsorption energy (E_{ad}) of TCNQ and TTF on the edges of the structures with and without chemical functionalization is calculated to study the effect of chemical functionalization on the adsorption ability of the finite graphene nanoribbon superlattices. We found that the adsorption energy is greatly enhanced by attaching COOH groups to the A120(2)L2 superlattice, as depicted in Fig. 4 (d), (e). Namely, for the adsorption of TTF (TCNQ) by A120(2)L2-COOH the adsorption energy increases from E_{ad}=1.5 (0.51) eV in the non-functionalized superlattices to 2.7 (0.53) eV in the functionalized ones. Similarly, in Z120(3)L2 clusters the adsorption energy of TTF/TCNQ increases from E_{ad}=1.47/0.34 eV in the non-functionalized cluster to 2.33/2.01 eV when it is functionalized with three NH2 groups. Hence, the adsorption ability can be significantly enhanced by attaching proposed chemical groups to the superlattices.

4. CONCLUSION

In summary, first principles calculations have been performed to investigate the electronic properties of graphene nanoribbon superlattices. The effects of finite length and chemical functionalization of such nanoribbon superlattices have been considered for armchair and zigzag edge termination. Seven chemical groups, namely CH3, CHO, CN, COCH3, COOH, NH2, and OH have been considered for the functionalization. It has been obtained that all the structures are stable before and after the chemical modification. The superlattices with armchair edges are characterized by a wide energy gap whereas those with zigzag ones have a narrow gap. The narrow energy gap arises from a pair of energy states localized at the opposite ends, i.e. in longitudinal direction rather than in transversal direction in conventional periodic structures. The effect of the superlattices length on the energy gap is negligible in armchair clusters while in zigzag the same increase in the length almost closes the energy gap. Additionally, in armchair the magnitude of the dipole moment increases by increasing the width whereas, in deep contrast, it oscillates in zigzag by increasing the width. The reason behind this peculiar difference is the arrangement of C-H bonds at the edges. At armchair edges the local dipoles from these C-H bonds sum up to increase the total electric dipole moment, while at zigzag edges local dipoles decrease the original value of the total dipole leading to oscillation of its value as a function of the superlattice width.

Chemical functionalization of the edges with such groups as COOH and NH2 significantly increases the total electric dipole moment of A120 and Z120 superlattices, respectively. However, other groups, like CH3 and OH, have a moderate effect on the total dipole moment. It is also found that the physical adsorption of tetracyanoquinodimethane on the edges of A120 superlattice decreases the energy gap from 2.66 eV to 0.25 eV, while that adsorption on edges of Z120 structure keeps the energy gap almost unaltered. The adsorption increases from 1.5 eV in non-functionalized A120 superlattice to 2.7 eV in COOH functionalized ones. The adsorption energy of the same molecules on the zigzag clusters also increases from 0.34 to 2.01 eV after attaching three NH2 groups to the edges of the Z120 superlattice. This shows graphene nanoribbon superlattices great potential for such applications as sensors and wastewater management. ***The current study demonstrates the effects of size, edge morphology, and chemical modification on the electronic and adsorption properties of single layer nanoribbon superlattices. A future research on this subject shall be studying the effects of these parameters on bilayer and multilayer structures which can exhibit new electronic features and provide additional enhancement of sensing properties.***

ACKNOWLEDGMENTS

This research utilized Imam Abdulrahman Bin Faisal (IAU)'s Bridge HPC facility, supported by IAU Scientific and High Performance Computing Center. https://doi.org/10.5281/zenodo.1117442. VAS acknowledges funding by EU H2020 RISE project CoExAN (Grant No. H2020-644076) and support by the RCN through grant number 274853, and partly through its CoE funding scheme, project number 262633, "QuSpin".

REFERANCES

[1] L. Chen, L. He, H. S. Wang, H. Wang, S. Tang, C. Cong, H. Xie, L. Li, H. Xia, T. Li, T. Wu, D.

Zhang, L. Deng, T. Yu, X. Xie, and M. Jiang, Nat. Commun. **8**, 14703 (2017).
[2] I. Palacio, A. Celis, M. N. Nair, A. Gloter, A. Zobelli, M. Sicot, D. Malterre, M. S. Nevius, W. A. de Heer, C. Berger, E. H. Conrad, A. Taleb-Ibrahimi, and A. Tejeda, Nano Lett. **15**, 182 (2015).
[3] L. Tapasztó, G. Dobrik, P. Lambin, and L. P. Biró, Nat. Nanotechnol. **3**, 397 (2008).
[4] G. Wang, S. Wu, T. Zhang, P. Chen, X. Lu, S. Wang, D. Wang, K. Watanabe, T. Taniguchi, D. Shi, R. Yang, and G. Zhang, Appl. Phys. Lett. **109**, (2016).
[5] J. Cai, P. Ruffieux, R. Jaafar, M. Bieri, T. Braun, S. Blankenburg, M. Muoth, A. P. Seitsonen, M. Saleh, X. Feng, K. Müllen, and R. Fasel, Nature **466**, 470 (2010).
[6] M. Khandelwal and A. Kumar, J. Mater. Chem. A **3**, 22975 (2015).
[7] T. J. Sisto, Y. Zhong, B. Zhang, M. T. Trinh, K. Miyata, X. Zhong, X.-Y. Zhu, M. L. Steigerwald, F. Ng, and C. Nuckolls, J. Am. Chem. Soc. **139**, 5648 (2017).
[8] L. Liang and V. Meunier, Phys. Rev. B **86**, 195404 (2012).
[9] E. Costa Girão, L. Liang, E. Cruz-Silva, A. G. S. Filho, and V. Meunier, Phys. Rev. Lett. **107**, 135501 (2011).
[10] S. Wang and J. Wang, J. Phys. Chem. C **116**, 10193 (2012).
[11] E. C. Girão, E. Cruz-Silva, and V. Meunier, ACS Nano **6**, 6483 (2012).
[12] X. Wu and X. C. Zeng, Nano Res. **1**, 40 (2008).
[13] X. Li, X. Wang, L. Zhang, S. Lee, and H. Dai, Science (80-.). **319**, 1229 (2008).
[14] N. T. Cuong, M. Otani, and S. Okada, Phys. Rev. B **87**, 45424 (2013).
[15] V. A. Saroka, K. G. Batrakov, and L. A. Chernozatonskii, Phys. Solid State **56**, 2135 (2014).
[16] V. A. Saroka, K. G. Batrakov, V. A. Demin, and L. A. Chernozatonskii, J. Phys.: Condens. Matter **27**, 145305 (2015).
[17] V. A. Saroka and K. G. Batrakov, Russ. Phys. J. **59**, 633 (2016).
[18] D. Szczęśniak, A. P. Durajski, A. Khater, and D. Ghader, EPL (Europhysics Lett. **114**, 48001 (2016).
[19] P. Han, K. Akagi, F. Federici Canova, H. Mutoh, S. Shiraki, K. Iwaya, P. S. Weiss, N. Asao, and T. Hitosugi, ACS Nano **8**, 9181 (2014).
[20] D. G. de Oteyza, A. García-Lekue, M. Vilas-Varela, N. Merino-Díez, E. Carbonell-Sanromà, M. Corso, G. Vasseur, C. Rogero, E. Guitián, J. I. Pascual, J. E. Ortega, Y. Wakayama, and D. Peña, ACS Nano **10**, 9000 (2016).
[21] V. A. Saroka, H. Abdelsalam, V. A. Demin, D. Grassano, S. A. Kuten, A. L. Pushkarchuk, O. Pulci, Semiconductors 52, 1890 (2018).
[22] N. Merino-Díez, J. Li, A. Garcia-Lekue, G. Vasseur, M. Vilas-Varela, E. Carbonell-Sanroma, M. Corso, J. E. Ortega, D. Peña, J. I. Pascual, and D. and G. de Oteyza, J. Phys. Chem. Lett. 9, 25 (2018).
[23] P. S. Costa, J. D. Teeter, A. Enders, and A. Sinitskii, Carbon N. Y. 134, 310 (2018).
[24] T. H. Vo, M. Shekhirev, D. A. Kunkel, M. D. Morton, E. Berglund, L. Kong, P. M. Wilson, P. A. Dowben, A. Enders, and A. Sinitskii, Nat. Commun. **5**, 3189 (2014).
[25] A. Radocea, T. Sun, T. H. Vo, A. Sinitskii, N. R. Aluru, and J. W. Lyding, Nano Lett. **17**, 170 (2017).
[26] M. Mehdi Pour, A. Lashkov, A. Radocea, X. Liu, T. Sun, A. Lipatov, R. A. Korlacki, M. Shekhirev, N. R. Aluru, J. W. Lyding, V. Sysoev, and A. Sinitskii, Nat. Commun. **8**, 820 (2017).
[27] A. Narita, X. Feng, Y. Hernandez, S. A. Jensen, M. Bonn, H. Yang, I. A. Verzhbitskiy, C. Casiraghi, M. R. Hansen, A. H. R. Koch, G. Fytas, O. Ivasenko, B. Li, K. S. Mali, T. Balandina, S. Mahesh, S. De Feyter, and K. Müllen, Nat. Chem. **6**, 126 (2014).
[28] H. Li, L. Wang & X.Zhai, Sci. Rep. 6, 36651(2016)
[29] S.-X. Xia, X. Zhai, Y. Huang, J.-Q. Liu, L.-L. Wang, S.-C. Wen, Opt. Lett. 42, 3052 (2017).
[30] H. Li, C. Ji, Y. Ren, J. Hu, M. Qin, L. Wang, Carbon 141, 481 (2019).
[31] J. Cai, C. A. Pignedoli, L. Talirz, P. Ruffieux, H. Söde, L. Liang, V. Meunier, R. Berger, R. Li, X. Feng, K. Müllen, R. Fasel, Nat. Nanotechnol. 9, 896 (2014).
[32] F. Khoeini, Superlattices Microstruct. 81, 202 (2015).

[33] P. Jangida, D. Pathana, A. Kottantharayila, Carbon 132, 65 (2018).
[34] Y. Lee, F. Zhao, T. Cao, J. Ihm, and S. G. Louie, Nano Lett. 18, 7247 (2018).
[35] V. A. Saroka and K. G. Batrakov, in *Physics, Chem. Appl. Nanostructures*, edited by V. E. Borisenko, S. V. Gaponenko, V. S. Gurin, and C. H. Kam (World Scientific, 2015), pp. 240–243.
[36] V. Saroka, (2017, August 3). "Zigzag-Shaped Graphene Nanoribbons," Wolfram Demonstrations Project [Online]. Available: http://demonstrations.wolfram.com/ZigzagShapedGrapheneNanoribbons/
[37] V. A. Saroka, A. L. Pushkarchuk, S. A. Kuten, and M. E. Portnoi, J. Saudi Chem. Soc. **22**, 985 (2018).
[38] M.J. Frisch, G.W. Trucks, H.B. Schlegel, et al., GAUSSIAN 09, Revision A.1, Gaussian, Inc., Wallingford, CT, 2009.
[39] P. Hohenberg, W. Kohn, Phys. Rev. **136**, 864 (1964).
[40] W. Kohn, L.J. Sham, Phys. Rev. **140**,1133 (1965).
[41] A. D. Becke, J. Chem. Phys. **98,** 5648 (1993).
[42] C. Lee, W. Yang, P.G. Parr, Phys. Rev. B **37**,785 (1998).
[43] H. Zheng and W. Duley, Phys. Rev B **78**, 045421 (2008).
[44] H. Abdelsalam, H. Elhaes, M. A. Ibrahim, Physica B Condens Matter. **537**, 77 (2018).
[45] Y.-W. Son, M. L. Cohen, and S. G. Louie, Phys. Rev. Lett. **97**, 216803 (2006).
[46] H. Abdelsalam, T. Espinosa-Ortega, I. Lukyanchuk, Low Temp. Phys. **41**, 396 (2015).
[47] K. Wakabayashi, K.-I. Sasaki, T. Nakanishi, and T. Enoki, Sci. Technol. Adv. Mater. **11**, 54504 (2010).
[48] V. A. Saroka, M. V. Shuba, and M. E. Portnoi, Phys. Rev. B **95**, 155438 (2017).
[49] H. Abdelsalam, H. Elhaes, M. A. Ibrahim, Chem. Phys. Lett. **696**, 138 (2018).
[50] I. S. S. de Oliveira and R. H. Miwa, J. Appl. Phys.**142**, 044301 (2015).
[51] Y. Jing, Q. Tang, P. He, Z. Zhou and P. Shen, Nanotechnology **26**, 095201 (2015).

Highlights

- The electronic properties of finite graphene nanoribbons superlattices are investigated before and after chemical functionalization.
- The electronic properties are strongly depend on the superlattices edge termination and chemical modification.
- The superlattices with zigzag edge are characterized by tiny energy gap while the ones with armchair termination have a wide gap.
- The total dipole moment increase by increasing the superlattice width in armchair flakes while in zigzag-shaped ones it oscillates in magnitude and direction.
- The adsorption energy of small organic molecules, such as tetrathiafulvalene, significantly increases by chemical functionalization.